Supporting Information

for

Plasma-Enhanced Atomic Layer Deposition of $AlPO_4$/AlP_xO_y: Comparing Dual Source and Supercycle Approaches for Composition Control

Florian Preischel[a,b], David Zanders[a], Jean-Pierre Glauber[a,b], Karl Rönnby[c], Detlef Rogalla[d], Thomas Gemming[b], Peter Dement,[b] Michal Nolan,[c] Anjana Devi[a,b,e,f]*

[a] Inorganic Materials Chemistry, Ruhr University Bochum, Universitätsstr. 150, 44801 Bochum, Germany
[b] Leibniz Institute for Solid State and Materials Research, Helmholtzstr. 20, 01069 Dresden, Germany
[c] Tyndall National Institute, Lee Maltings, University College Cork, Cork T12 R5CP, Ireland
[d] RUBION, Ruhr University Bochum, Universitätsstr. 150, 44801 Bochum, Germany
[e] Fraunhofer Institute for Microelectronic Circuits and Systems (IMS), Finkenstr. 61, Duisburg, Germany
[f] Chair of Materials Chemistry, TU Dresden, Bergstr. 66, 01069 Dresden, Germany

Contents

Synthesis and characterization of TMA phosphorous adducts and $P(NMe_2)_3$ (^1H and ^{13}C NMR, TG, LIFDI MS)

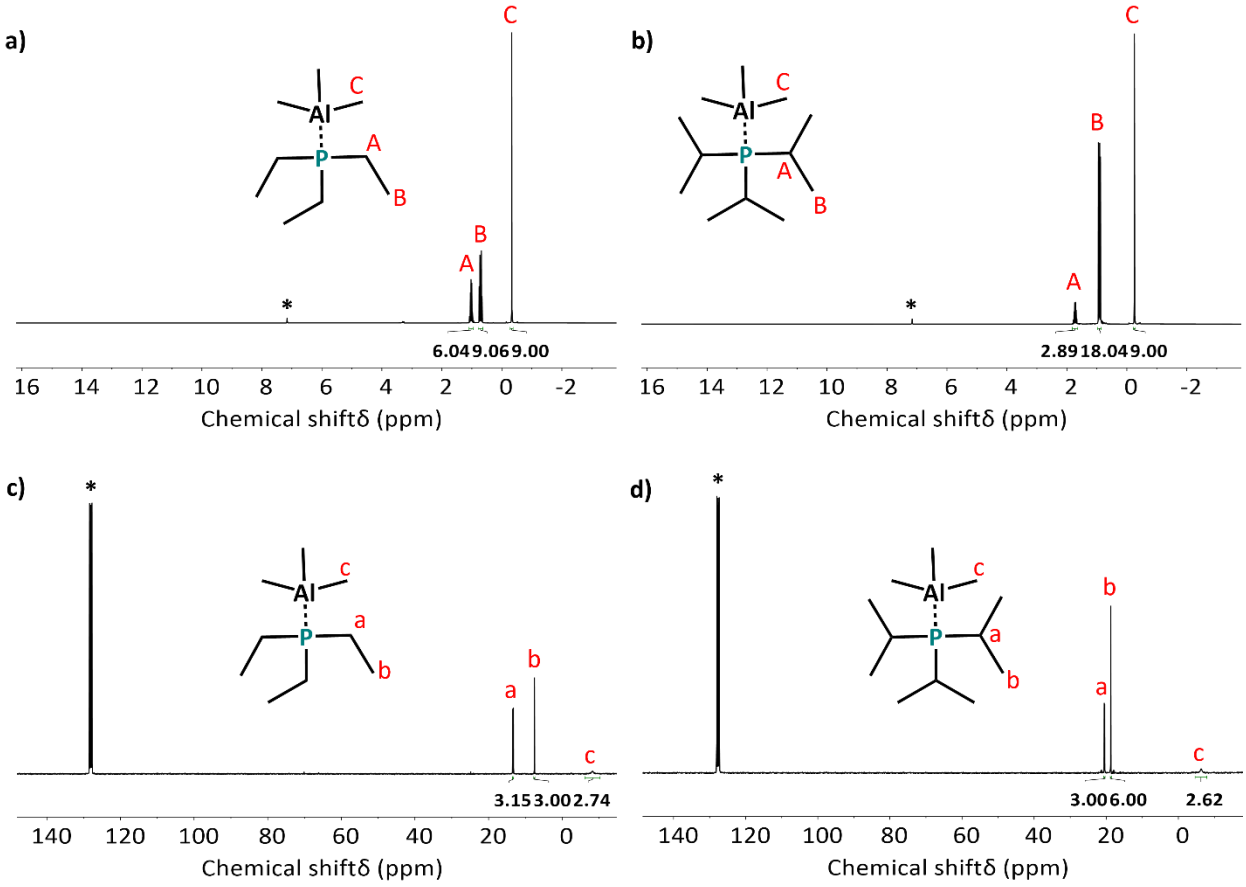

Figure S1. Full ^1H (top) and ^{13}C NMR (bottom) spectra of TMAPET (**a**, **c**) and TMAPIP (**b**, **d**) with assigned peaks. All spectra are recorded in benzene-d_6 (marked with an asterisk).

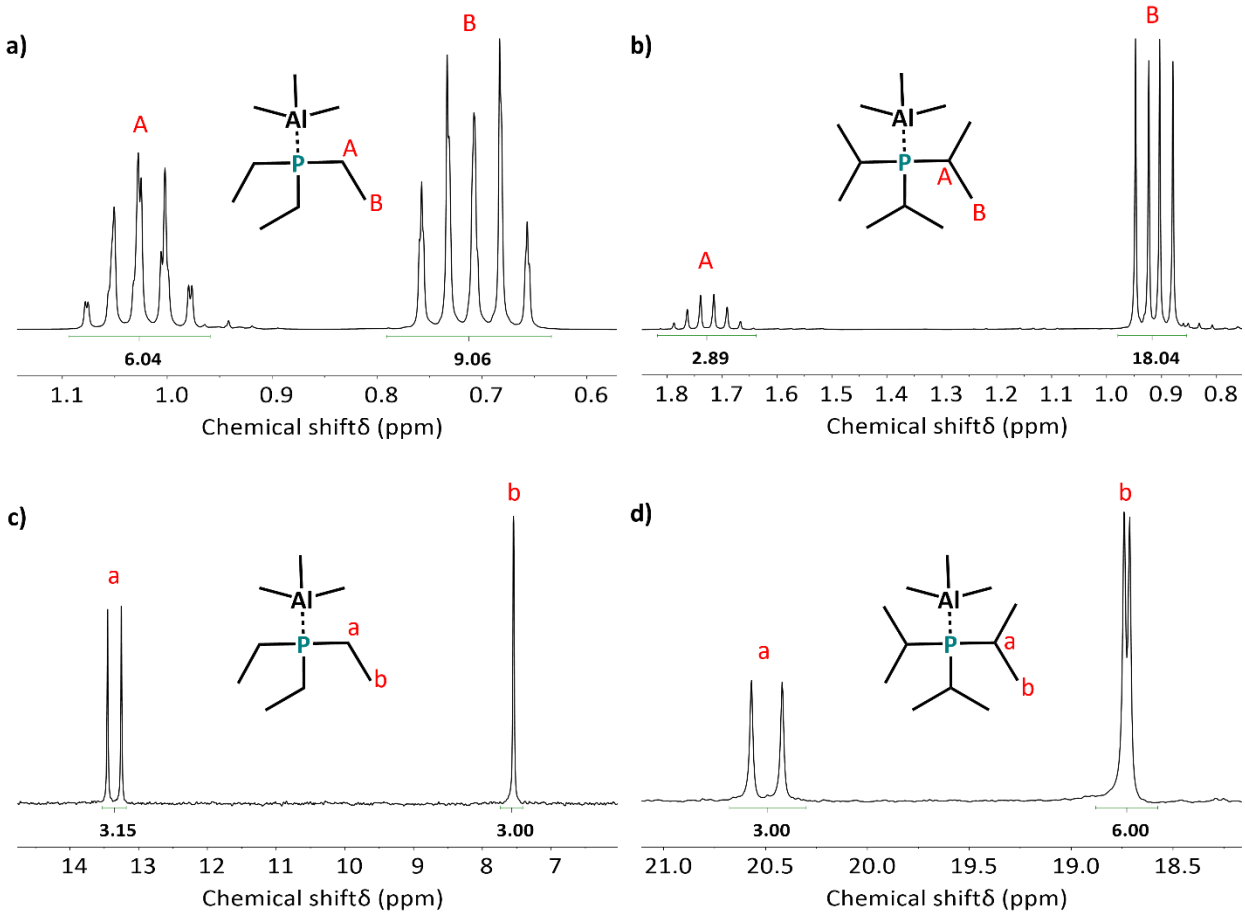

Figure S2. ^{1}H (top) and ^{13}C NMR (bottom) spectra of TMAPET (**a**, **c**) and TMAPIP (**b**, **d**) with a zoom into the region of signals originating from the P-adducts. All spectra are recorded in benzene-d_6.

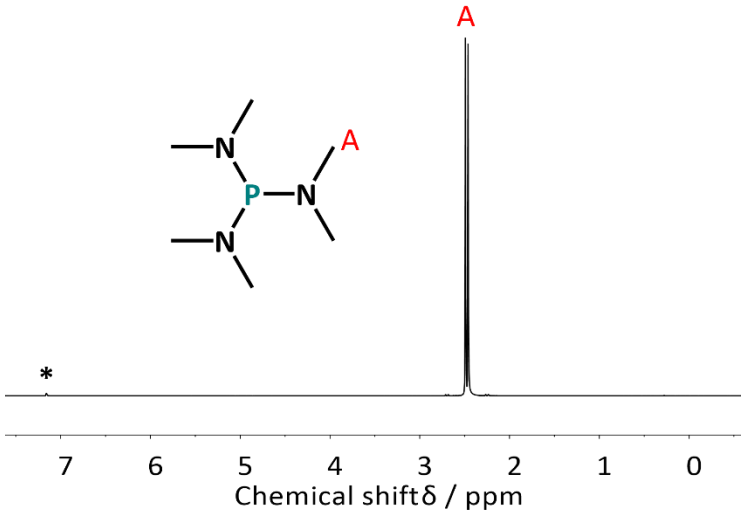

Figure S3. ^{1}H NMR of $P(NMe_2)_3$, recorded in benzene-d_6 (marked with an asterisk).

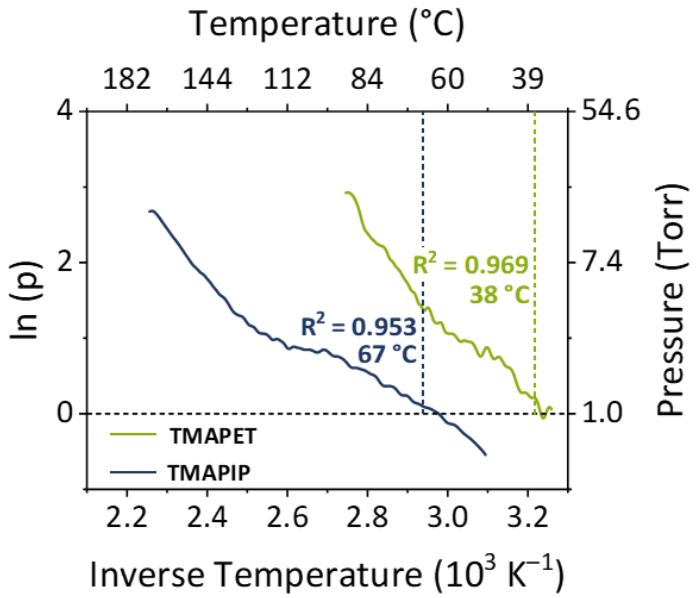

Figure S4. Clausius-Clapeyron plots of TMAPET (green) and TMAPIP (blue), derived from DTG data.

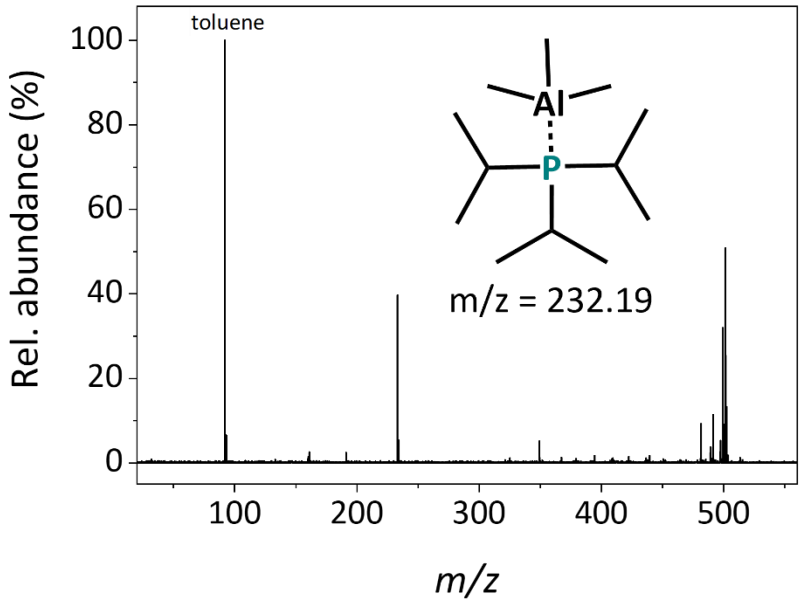

Figure S5. LIFDI-MS spectrum of TMAPIP recorded in toluene.

PEALD process development for AlP_xO_y thin films using TMAPIP and O_2 plasma at 120 °C

Compositional analysis of AlP_xO_y thin films using RBS/NRA

For all samples on Si, the Al concentration must be considered a qualitative approximation, as the Al peak overlaps with the broad Si signal from the substrate in RBS and cannot be determined by NRA.

For better comparability, the stoichiometry from RBS/NRA results on GC has been calculated by normalizing the P and O concentrations relative to Al, yielding the composition as $Al_1P_xO_y$.

Table S1. Composition of AlP_xO_y thin films deposited on Si using TMAPIP.

TMAPIP pulse (ms)	C (at.%)	N (at.%)	O (at.%)	Al (at.%)	P (at.%)
150	1.6	1.4	67.8	25.7	3.6
300	0.7	0.1	59.5	36.5	3.2
500	1.2	0.0	67.0	28.8	3.0

Table S2. Composition of AlP_xO_y thin films deposited on GC using TMAPIP and the derived stoichiometry.

TMAPIP pulse (ms)	N (at.%)	O (at.%)	Al (at.%)	P (at.%)	AlP_xO_y	
					x	y
150	0.0	64.9	31.6	3.5	0.11	2.05
300	0.0	64.8	32.1	3.1	0.10	2.01
500	0.0	65.6	30.6	3.8	0.12	2.14

PEALD process development for AlP_xO_y thin films using supercycles of TMA and $P(NMe_2)_3$ with O_2 plasma

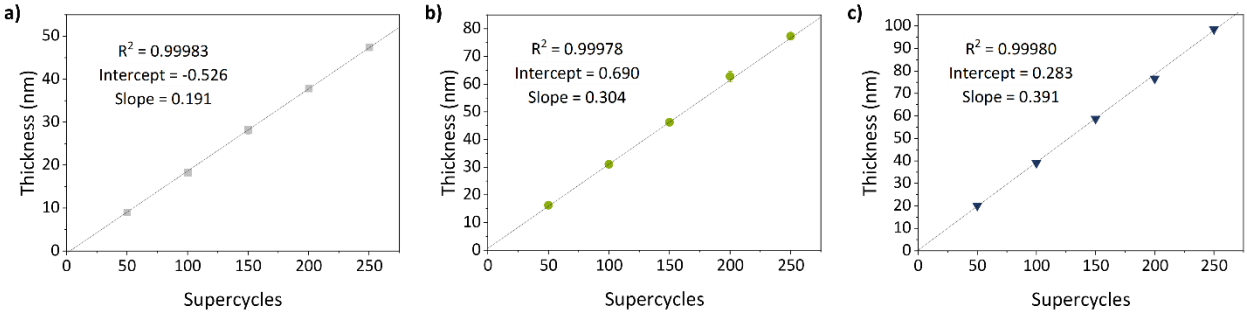

Figure S6. Linearity of thickness versus the number of PEALD supercycles, consisting of **a)** A+B, **b)** 2A+B, and **c)** 3A+B, with a linear fit for each dataset.

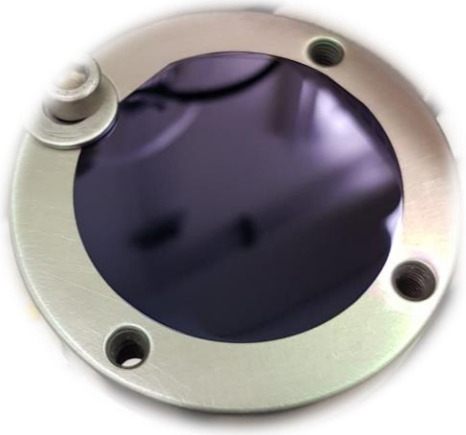

Figure S7. An image of a 2-inch Si wafer uniformly coated with 98.6 nm of AlP_xO_y using 250 SCs consisting of a 3A+B sequence at 150 °C.

Compositional analysis of AlP_xO_y thin films deposited at 150 °C using a supercycle with varying numbers of $P(NMe_2)_3$ (A) cycles and a single TMA (B) cycle with O_2 plasma performed by RBS/NRA

Table S3. Composition of AlP_xO_y thin films deposited on Si using supercycles of varying A cycles and one B cycle.

SC	C (at.%)	N (at.%)	O (at.%)	Al (at.%)	P (at.%)
A+B	0.9	0.0	66.1	19.2	13.8
2A+B	0.6	0.8	61.6	20.7	16.3
3A+B	0.3	1.0	63.9	16.5	18.3
4A+B	0.2	0.5	69.3	9.9	20.0

Table S4. Composition of AlP_xO_y thin films deposited on GC using supercycles of varying A cycles and one B cycle, and the derived stoichiometry.

SC	N (at.%)	O (at.%)	Al (at.%)	P (at.%)	AlP_xO_y	
					x	y
A+B	0.3	66.8	20.5	12.4	0.60	3.25
2A+B	1.5	65.9	15.2	17.5	1.15	4.34
3A+B	0.6	67.5	12.8	19.1	1.49	5.26
4A+B	0.8	68.9	10.6	19.7	1.86	6.50

Compositional analysis of AlP_xO_y thin films deposited at different temperatures using a supercycle that alternates between one $P(NMe_2)_3$ (A) cycle and one TMA (B) cycle with O_2 plasma by RBS/NRA

Table S5. Composition of AlP_xO_y thin films deposited on Si using a supercycle of one A cycle and one B cycle.

T_{dep} (°C)	C (at.%)	N (at.%)	O (at.%)	Al (at.%)	P (at.%)
60	0.7	0.2	53.4	39.1	6.6
80	0.6	0.0	57.9	32.4	9.1
100	0.5	0.0	57.8	31.9	9.8
125	0.6	0.0	55.6	33.1	10.7
150	0.9	0.0	66.1	19.2	13.8
175	0.5	1.0	52.5	34.8	11.2
200	0.5	0.3	60.9	24.4	13.9
220	0.7	0.2	60.5	24.8	13.8
240	0.3	0.0	60.0	26.9	12.8

Table S6. Composition of AlP_xO_y thin films deposited on GC using a supercycle with one A cycle and one B cycle, along with the derived stoichiometry.

T_{dep} (°C)	N (at.%)	O (at.%)	Al (at.%)	P (at.%)	AlP_xO_y	
					x	y
60	0.7	67.0	24.7	7.6	0.31	2.72
80	0.8	67.1	22.8	9.3	0.41	2.94
100	0.5	66.8	22.2	10.6	0.48	3.01
125	0.7	67.2	20.6	11.6	0.56	3.27
150	0.3	66.8	20.5	12.4	0.60	3.25
175	0.6	67.2	19.5	12.7	0.65	3.44
200	0.7	66.7	19.5	13.2	0.68	3.43
220	07	67.3	18.1	13.9	0.77	3.72
240	0.7	67.9	18.5	12.9	0.70	3.67

Compositional analysis of AlP_xO_y thin films deposited at different temperatures using a supercycle that alternates between two $P(NMe_2)_3$ (A) cycles and one TMA (B) cycle with O_2 plasma by RBS/NRA

Table S7. Composition of AlP_xO_y thin films deposited on Si using a supercycle of two A cycles and one B cycle.

T_{dep} (°C)	C (at.%)	N (at.%)	O (at.%)	Al (at.%)	P (at.%)
60	0.5	0.3	63.0	21.6	14.6
80	0.5	0.0	58.5	26.8	14.2
100	0.4	0.8	58.7	25.5	14.7
125	0.3	0.0	61.1	23.4	15.1
150	0.3	0.0	59.1	25.4	15.1
175	0.5	0.0	64.3	17.4	17.8
200	0.3	0.0	565	28.6	14.6
220	0.3	0.6	62.9	20.8	15.4
240	0.4	0.9	60.9	22.4	15.4

Table S8. Composition of AlP_xO_y thin films deposited on GC using a supercycle with two A cycles and one B cycle, along with the derived stoichiometry.

T_{dep} (°C)	N (at.%)	O (at.%)	Al (at.%)	P (at.%)	AlP_xO_y	
					x	y
60	0.8	67.7	16.7	14.8	0.88	4.05
80	1.2	67.4	15.4	16.0	1.04	4.37
100	0.6	69.0	15.1	15.3	1.01	4.56
125	0.8	69.8	14.4	15.0	1.04	4.84
150	0.5	69.2	14.7	15.5	1.05	4.70
175	1.1	67.0	16.1	15.7	0.98	4.16
200	0.8	68.0	15.3	15.9	1.04	4.44
220	0.7	67.5	16.2	15.6	0.96	4.16
240	1.3	70.7	11.6	16.5	1.42	6.11

Compositional analysis of AlP_xO_y thin films deposited at different temperatures using a supercycle that alternates between three $P(NMe_2)_3$ (A) cycles and one TMA (B) cycle with O_2 plasma by RBS/NRA

Table S9. Composition of AlP_xO_y thin films deposited on Si using a supercycle of three A cycles and one B cycle.

T_{dep} (°C)	C (at.%)	N (at.%)	O (at.%)	Al (at.%)	P (at.%)
60	0.4	0.4	65.4	16.2	17.6
80	0.4	0.3	65.7	15.9	17.7
100	0.4	0.0	65.5	15.7	18.4
125	0.2	1.1	64.7	15.6	18.5
150	0.2	0.7	66.3	14.0	18.8
175	0.3	0.0	65.9	15.0	18.7
200	0.2	0.6	72.1	5.8	21.2
220	0.4	0.2	65.0	14.5	19.9
240	0.4	0.9	67.7	10.9	20.1

Table S10. Composition of AlP_xO_y thin films deposited on GC using a supercycle with three A cycles and one B cycle, along with the derived stoichiometry.

T_{dep} (°C)	N (at.%)	O (at.%)	Al (at.%)	P (at.%)	AlP_xO_y	
					x	y
60	0.5	68.2	14.9	16.4	1.10	4.57
80	0.7	66.8	15.2	17.3	1.14	4.41
100	0.8	67.1	14.4	17.7	1.23	4.66
125	0.8	67.6	13.5	18.1	1.34	5.00
150	0.6	67.5	12.8	19.1	1.49	5.26
175	0.4	67.7	12.5	19.4	1.55	5.41
200	0.2	68.4	11.0	20.3	1.84	6.20
220	0.5	67.9	11.1	20.5	1.85	6.13
240	0.2	69.8	10.1	20.0	1.98	6.93

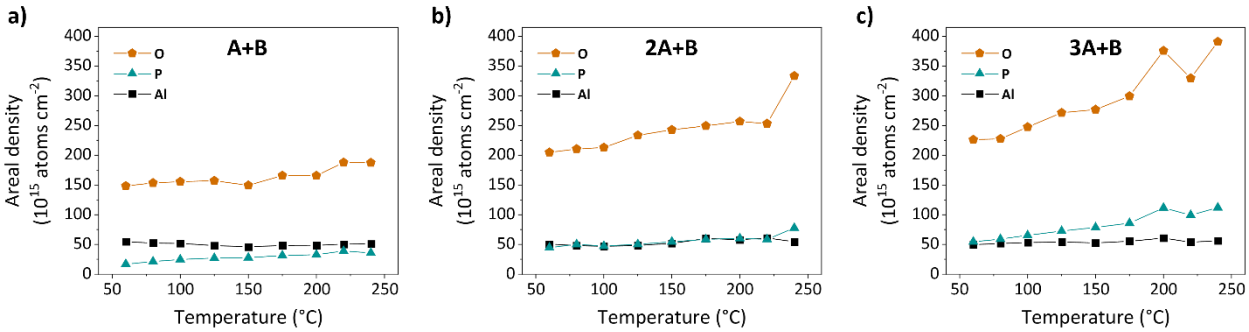

Figure S8. Absolute areal densities of O, P, and Al atoms in AlP_xO_y thin films deposited on GC using a supercycle of **a)** one, **b)** two, and **c)** three A cycles alternating with one B cycle, as determined by RBS.

Table S11. Stoichiometry of as-deposited AlP_xO_y thin films on GC using a supercycle with varying A cycles and one B cycle at different temperatures compared to the respective annealed layer. For better comparability, the stoichiometry has been normalized to an Al ratio of 1.

T_{dep} (°C)	SC	AlP_xO_y	
		x	y
150	**2A+B**	1.15	4.34
annealed		0.57	3.40
60	**3A+B**	1.10	4.57
annealed		1.12	4.85
100	**3A+B**	1.23	4.66
annealed		1.27	4.92
200	**3A+B**	1.84	6.20
annealed		1.78	5.98

Characterization of AlP_xO_y thin films deposited on Si using PEALD supercycles (XRD, XPS, AFM, TEM)

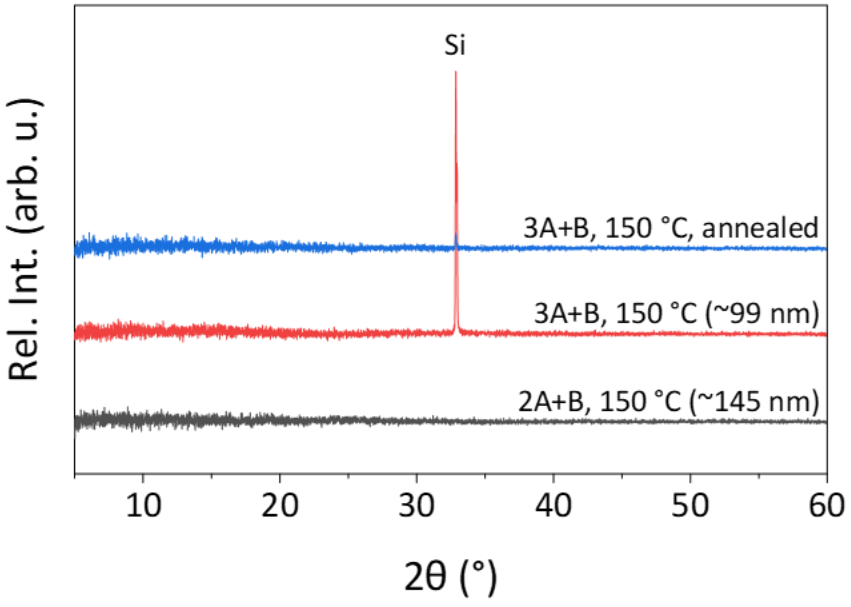

Figure S9. XRD of AlP_xO_y layers as deposited on Si at 150 °C using 500 2A+B SCs and 150 3A+B SCs, and after annealing at 600 °C.

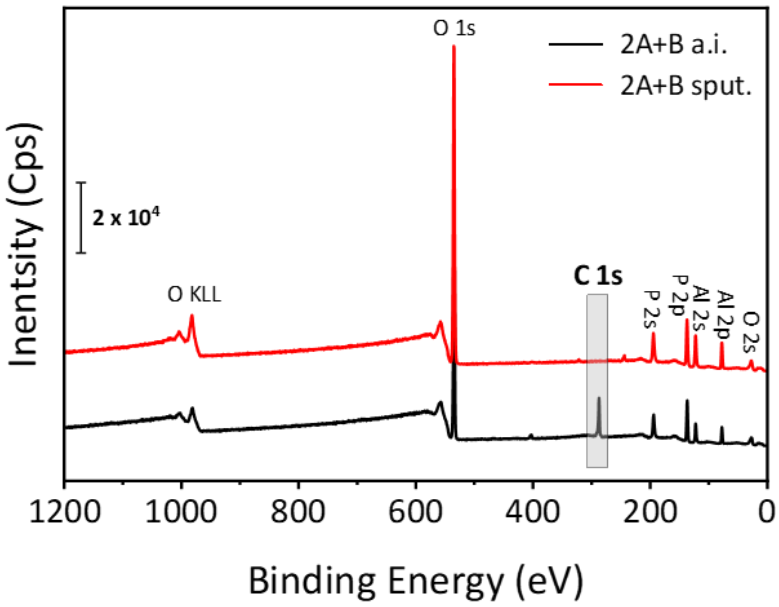

Figure S10. XPS survey spectra of as-introduced and sputtered surfaces of $AlPO_4$ deposited on Si with 150 SCs using a 2A+B sequence at 150 °C. The C1s core-level region is highlighted, showing the disappearance of the carbon peak after sputtering.

Table 12. Al 2p, P 2p, and O 1s binding energies and their respective component shares obtained from XPS measurements of as-introduced $AlPO_4$ thin films deposited on Si with 150 SCs using varying SC sequences at 150 °C.

SC	Binding energy (eV)			Component share (%)		
	Al 2p	P 2p	O 1s	Al 2p	P 2p	O 1s
A+B	74.86	134.28	532.12	29.8	18.5	51.7
2A+B	75.55	134.86	532.72	20.8	26.2	53.1
3A+B	76.08	135.42	533.23	16.8	28.2	55.1
4A+B	76.34	135.71	533.51	15.8	29.4	54.8

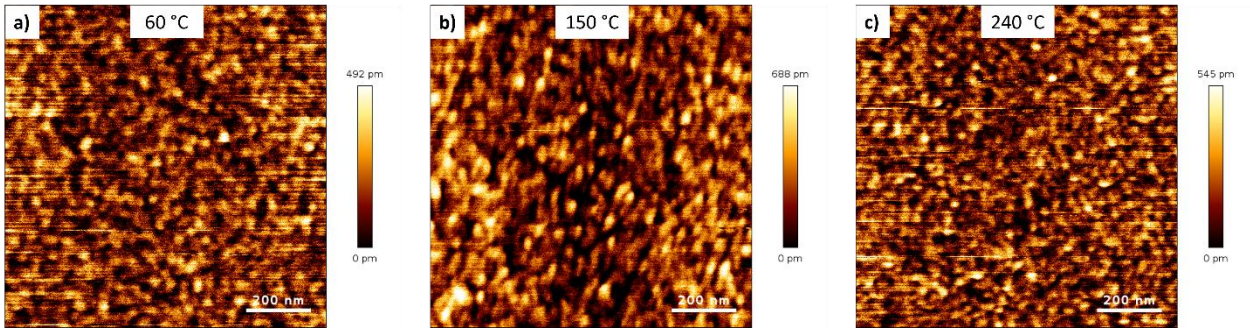

Figure S11. AFM images of AlP_xO_y deposited on Si with 150 A+B supercycles at **a)** 60 °C, **b)** 150 °C, and **c)** 240 °C.

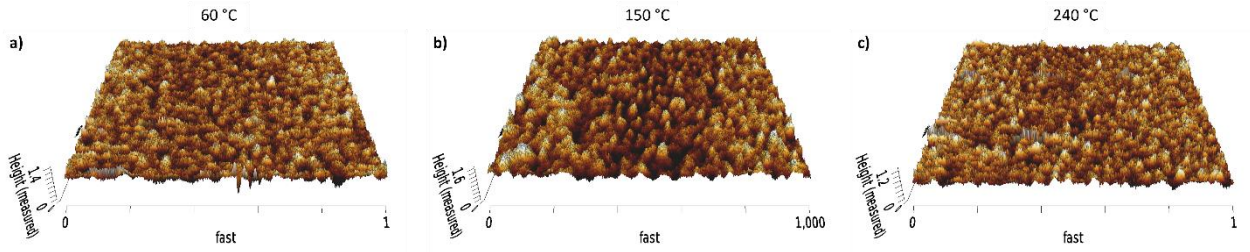

Figure S12. 3D view of AFM images of AlP_xO_y deposited on Si with 150 A+B supercycles at **a)** 60 °C, **b)** 150 °C, and **c)** 240 °C.

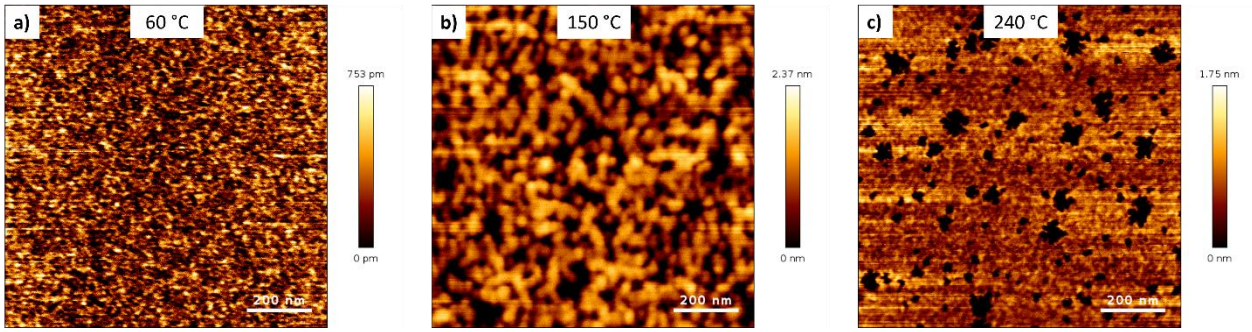

Figure S13. AFM images of AlP_xO_y deposited on Si with 150 2A+B supercycles at **a)** 60 °C, **b)** 150 °C, and **c)** 240 °C.

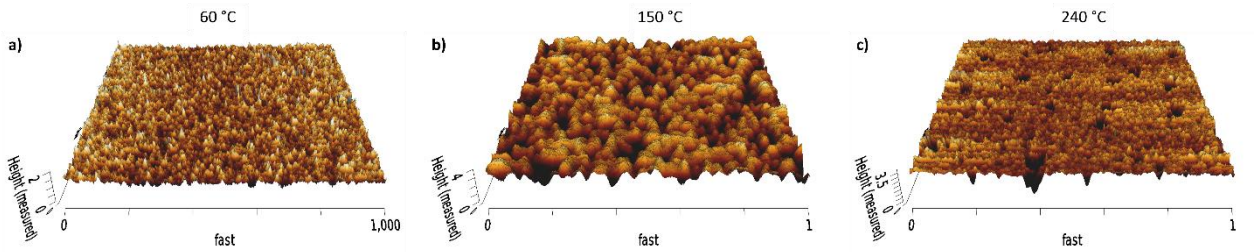

Figure S14. 3D view of AFM images of AlP_xO_y deposited on Si with 150 2A+B supercycles at **a)** 60 °C, **b)** 150 °C, and **c)** 240 °C.

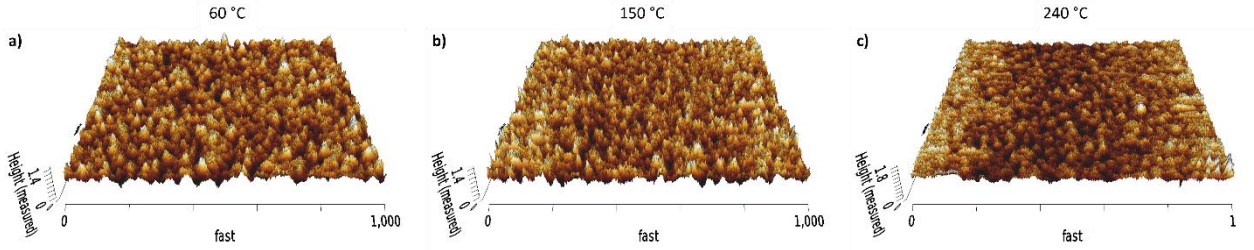

Figure S15. 3D view of AFM images of AlP_xO_y deposited on Si with 150 3A+B supercycles at **a)** 60 °C, **b)** 150 °C, and **c)** 240 °C.

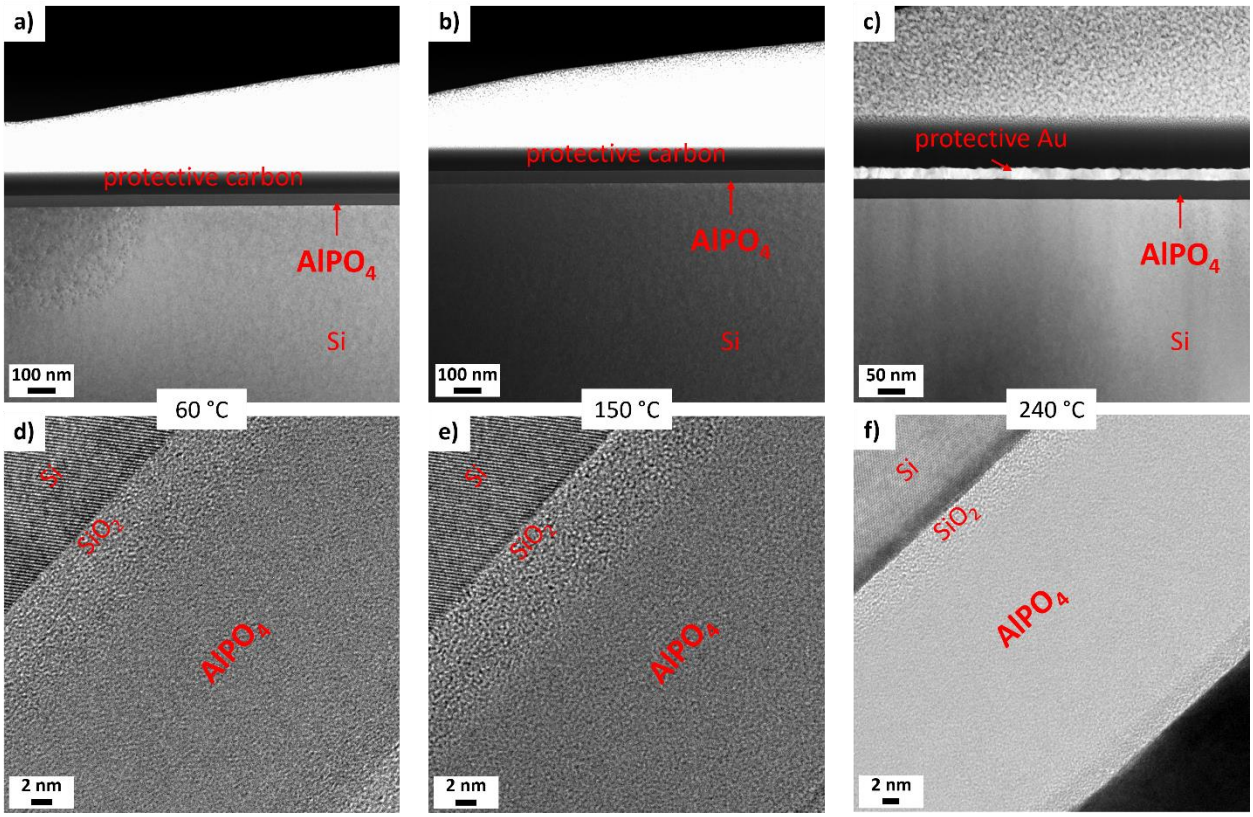

Figure S16. Overview of STEM images (top row) and HRTEM images (bottom row) of $AlPO_4$ deposited on Si with 150 2A+B supercycles at 60 °C (**a** and **d**), 150 °C (**b** and **e**), and 240 °C (**c** and **f**).

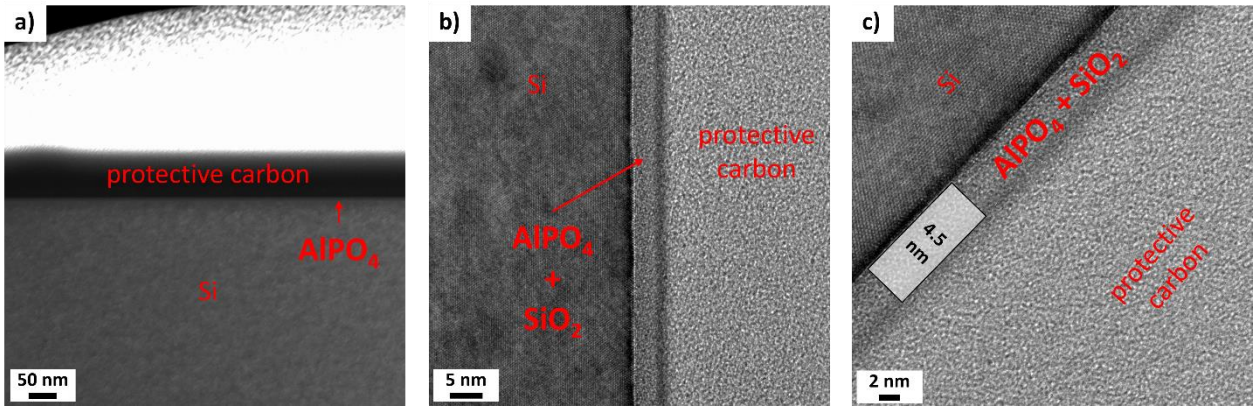

Figure S17. TEM images of $AlPO_4$ deposited on Si with 10 2A+B cycles at 150 °C. **a)** Shows an overview STEM image, while **b)** and **c)** display HRTEM images with the graphically derived thickness of the $AlPO_4$ layer.